Modelling passive cardiac conductivity during ischaemia

J. G. Stinstra[1,2] S. Shome[2,4] B. Hopenfeld[3] R. S. MacLeod[1,2,4]

[1]Scientific Computing & Imaging Institute, University of Utah, Salt Lake City, USA
[2]CardioVascular Research & Training Institute, University of Utah, Salt Lake City, USA
[3]National Heart, Lung & Blood Institute, National Institutes of Health, Bethesda, USA
[4]Department of Bioengineering, University of Utah, Salt Lake City, USA

Abstract—*The results of a geometric model of cardiac tissue, used to compute the bidomain conductivity tensors during three phases of ischaemia, are described. Ischaemic conditions were simulated by model parameters being changed to match the morphological and electrical changes of three phases of ischaemia reported in literature. The simulated changes included collapse of the interstitial space, cell swelling and the closure of gap junctions. The model contained 64 myocytes described by 2 million tetrahedral elements, to which an external electric field was applied, and then the finite element method was used to compute the associated current density. In the first case, a reduction in the amount of interstitial space led to a reduction in extracellular longitudinal conductivity by about 20%, which is in the range of reported literature values. Moderate cell swelling in the order of 10–20% did not affect extracellular conductivity considerably. To match the reported drop in total tissue conductance reported in experimental studies during the third phase of ischaemia, a ten fold increase in the gap junction resistance was simulated. This ten-fold increase correlates well with the reported changes in gap junction densities in the literature.*

Keywords—*Conductivity, Cardiac tissue, Bidomain, Ischaemia, Cardiac modelling, Gap junctions*

Med. Biol. Eng. Comput., 2005, **43**, 776–782

1 Introduction

ISCHAEMIA IS a state in which cells receive abnormally low amounts of nutrients. In the heart, ischaemia is typically caused by the partial or complete blockage of a coronary artery and is a precursor to a host of changes in cardiac tissue properties. Primary changes include alterations in myocyte (TRANUM-JENSEN *et al.*, 1981) and vascular morphology (KLÉBER and RIEGGER, 1987) and gap junction resistance (CARMELIET, 1999; KLÉBER and RIEGGER, 1987). Somewhat less significant changes occur in the conductivity of the interstitial space as a result of changes in the concentration of potassium ions due to ischaemia (YAN *et al.*, 1996).

Although there is substantial uncertainty regarding the effect of ischaemia on conductivity, there appear to be three phases of conductivity changes:

(a) immediately upon perfusion arrest, there is a substantial and sharp increase in longitudinal extracellular resistance (KLÉBER and RIEGGER, 1987; SMITH *et al.*, 1995)
(b) several minutes after perfusion arrest, a more gradual rise in longitudinal extracellular resistance lasts for at least 15 min (YAN *et al.*, 1996)
(c) overlapping the end of the second phase, a rapid rise in longitudinal intracellular resistance occurs approximately 15–30 min after perfusion arrest (SMITH *et al.*, 1995; JAIN *et al.*, 2003; KLÉBER and RIEGGER, 1987).

The above observations are also supported by studies reporting measurements of whole tissue (bulk) resistance during ischaemia (OWENS *et al.*, 1996; CINCA *et al.*, 1997). In these studies, although different species were used and ischaemia was sustained for different time periods, the time courses of changes in bulk resistance were similar.

Previous findings suggest several possible mechanisms for these three phases of ischaemia-induced conductivity changes. Following the arrest of coronary flow, an immediate increase in the extracellular longitudinal resistance of about 30% has been observed, which Kiéber and Riegger proposed was due to the collapse of capillaries after cardiac arrest (KLÉBER and RIEGGER, 1987). However, measurements by FLEISCHHAUER *et al.* (1995) suggest that the capillary system does not contribute to the overall extracellular conductivity, and thus a change in capillary volume would not be likely to alter the extracellular conductivity. Further support comes from our previous study, which showed that the conductivity of the capillary system is substantially lower than that of the interstitial space, because transverse currents have to pass in and out of the capillaries through a highly resistive capillary wall, and longitudinal currents have to flow around numerous red blood cells that almost completely clog the capillaries (STINSTRA *et al.*, 2005). Hence, we propose and evaluate in

Correspondence should be addressed to Dr Jeroen Stinstra; email: jeroen@cvrti.utah.edunicolas.chauveau@toulouse.inserm.fr
Paper received 15 June 2005 and in final form 22 August 2005
MBEC online number: 20054056

this study an alternative mechanism in which the immediate increase in longitudinal resistivity during the first phase is caused by a small but rapid decrease in the size of the interstitial space as fluid shifts from that space into the capillaries, because of the decrease in capillary hydrostatic pressure directly after perfusion arrest, and is drained out of the ischaemic zone.

The second phase of ischaemic conductivity, during which there is a more gradual rise in extracellular longitudinal resistance (SMITH *et al.*, 1995), occurs as a result of cell swelling, which initially decreases the volume of the interstitial space as fluid flows into the myocytes (YAN *et al.*, 1996). After the osmotic balance between the cell and the interstitial space is re-established, both the cell and the interstitial space may swell, with water being divided between those spaces according to their respective volumes, as the higher osmolality of the interstitial space draws water from more distant, non-ischaemic parts of the heart (TRANUM-JENSEN *et al.*, 1981). The proportional increase in both the intracellular and interstitial volumes probably does not greatly alter the bidomain conductivities, and the extent of cell swelling may depend on whether the ischaemia is low flow or no flow. In the case of no-flow ischaemia, metabolite washout is minimal, and so interstitial osmolyte accumulation at least partially balances intracellular accumulation, and only modest increases in cell volume may occur (WRIGHT and REES, 1998). In low-flow ischaemia, in contrast, washout of interstitial osmolytes would maintain an osmotic imbalance between the interstitial and intracellular spaces, resulting in greater cell swelling (WRIGHT and REES, 1998).

The third phase of resistance changes, a rapid increase in intracellular resistance, is probably attributable to the closing of gap junctions (SMITH *et al.*, 1995; OWENS *et al.*, 1996; JAIN *et al.*, 2003). According to BEARDSLEE *et al.* (2000), about 15 min after the blocking of perfusion to the myocardium, a considerable dephosphorylation of connexin-43 takes places, which leads to the closure of gap junctions. Furthermore, others have reported that prolonged ischaemia in isolated rabbit hearts resulted in the doubling of intracellular calcium concentration and a drop in intracellular pH to about 6.0 before a sharp rise in the bulk tissue resistance was observed (OWENS *et al.*, 1996). A recent study on cultured mouse astrocytes showed a correlation between prolonged intracellular acidification and the decoupling and internalisation of connexin-43 (DUFFY *et al.*, 2004). It is reasonable to extrapolate these findings to the cardiac domain, as cardiac tissue also contains connexin-43 and this supports the hypothesis that the sharp rise in intracellular resistance is a consequence of gap junction uncoupling.

Experimental studies have shown that the times of onset of different phases of arrhythmia correlate with the onset of changes in tissue impedances (SMITH *et al.*, 1995; CINCA *et al.*, 1997). A common way of studying the origin of arrhythmias in a three-dimensional substrate of myocardium is by using a computer model to simulate the effect of changes in the substrate, and these models are primarily based on changes in the driving currents across the myocyte membrane (SACHSE, 2004; HENRIQUEZ *et al.*, 2004; ROTH, 2004). One effect that is commonly not taken into account in these models, however, is the passive electrical conductivity changes that occur in ischaemic cardiac tissue. Cell swelling and the decoupling of gap junctions alter the microscopic structure of tissue and, hence, its passive electrical conductivity, and this change in conductivity will alter the volume conductor and thus the epicardial potentials. A recent modelling study by HOPENFELD *et al.* (2004; 2005) showed that the electrical anisotropy ratio of cardiac tissue and changes in its electrical conductivity influence the distribution of epicardial potentials. Hence, changes in tissue properties due to, for example, ischaemia will lead to changes in potential distributions.

The difficulty of modelling the changes in passive electrical properties lies in estimating the conductivity values of ischaemic tissue, as measurements are sparse and are often hard to interpret. Moreover, models are often based on the bidomain equations, which split the conductivity tensor into two parts, an extracellular component and an intracellular one. However, most conductivity measurements, even under ischaemic conditions, represent a weighted average of both tensors. Hence, to separate these components, a modelling approach is required that takes into account the detailed structure at a cellular level, as ischaemia influences the passive electrical properties at a cellular level. This model then can be used to couple the underlying physiological changes in ischaemia to the averaged electrical properties that are used in continuous modelling approaches, such as the bidomain model.

In a related study (STINSTRA *et al.*, 2004; 2005), we created a geometric model of cardiac tissue to compute the conductivity of cardiac tissue under healthy conditions. This model described the geometry of cardiac tissue at a cellular level and computed the currents flowing through this tissue, from which we determined the apparent bidomain conductivities. The aim of this study was to extend this model to ischaemic tissue and then compare the results with the few measurements reported in the literature.

2 Methods

2.1 *Conductivity model*

The computations of the effective passive conductivity of cardiac tissue were based on a geometric model of a piece of cardiac tissue described at a cellular level. The model consisted of two domains, the intracellular space (ICS) of the myocytes and the extracellular space (ECS) surrounding the myocytes, separated by the cell membrane. The ECS domain was subdivided into interstitial space (the space between neighbouring cells) and the capillary network. Previous simulations suggested that the resistance of the capillary network is significantly different from that of the interstitial space (STINSTRA *et al.*, 2005) and, hence, the ECS domain included a separate capillary compartment. Similarly, the ICS domain contained one compartment of intracellular fluid and another representing the gap junctions connecting the various myocytes. The conductivities of both the intracellular and extracellular fluids were assumed to be homogeneous and ohmic. In the model, the myocyte dimensions were roughly $10 \times 25 \times 100$ μm, and all the cells had their long axis aligned along the same longitudinal fibre direction.

The actual geometric model itself was generated using a computer algorithm that assigns a rule-based random shape to each myocyte in the model. The goal of this approach was to scrutinise the dependence of the model on general tissue properties, such as cell size and the overall size of the extracellular space, and not on the actual shape of every individual myocyte. Simulations under healthy conditions already demonstrated that the apparent conductivity is more dependent on the 'global' tissue properties than on the actual shape of each myocyte (STINSTRA *et al.*, 2005). Hence, we used the same approach for ischaemic tissue. Each set of global parameters is an average of the results of ten different cellular layouts that were randomly generated, where only the individual cell shapes were changed, and the overall properties of the tissue, such as average cell-to-cell distance and overall volume fractions, were kept the same.

The process of generating the tissue mesh is shown in Fig. 1 and consisted of turning a regular mesh consisting of hexagonal

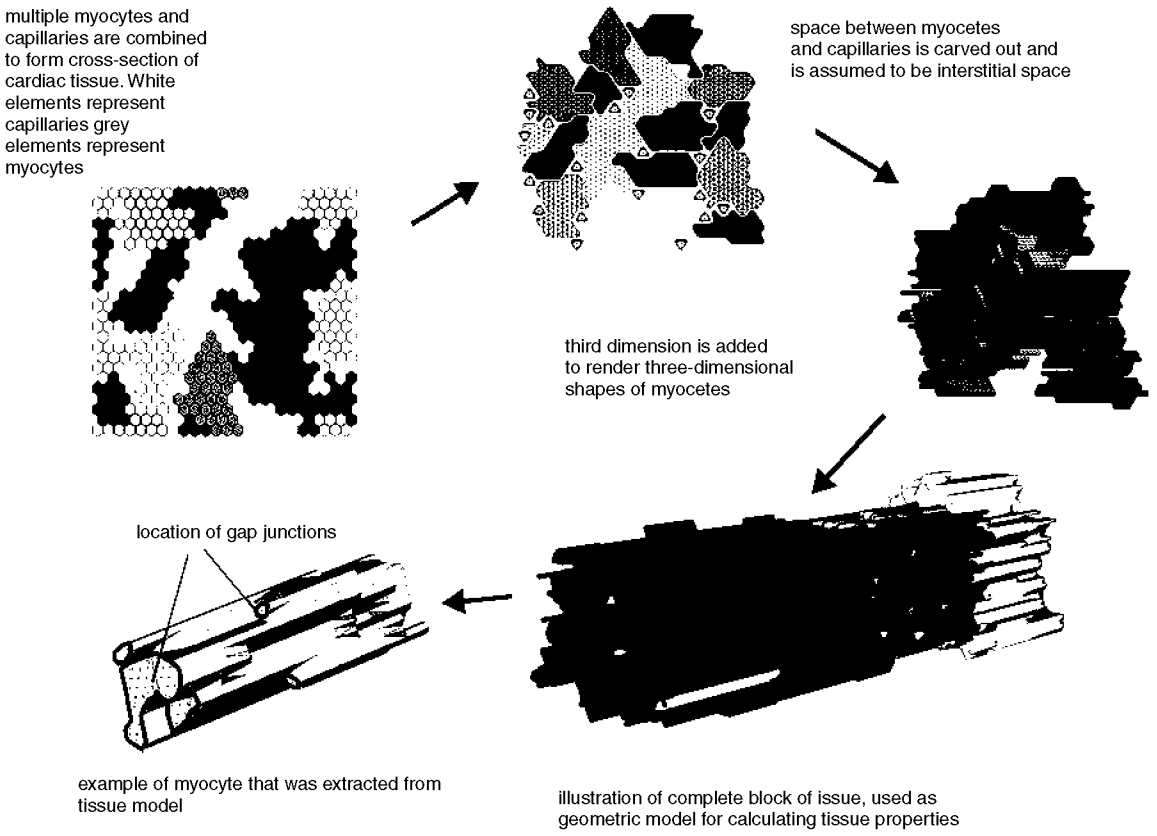

Fig. 1 *Process used to create geometric model of cardiac tissue*

cross-sectional elements into a three-dimensional model of myocytes embedded in an extracellular mesh of interstitial space and capillaries, as we have described previously (STINSTRA *et al.*, 2005). The process starts with building a random cross-section of a myocyte out of hexagons. Subsequently, more hexagons are added to form a full cross-section. In this process, capillaries are assigned as well, interspersed with the myocytes. In the next phase, a certain amount of extracellular space is added between the myocytes, and the myocytes are given a third dimension by extension of the hexagonal column in the fibre direction. As the latter process is random, the resulting myocyte shapes have the spiky look often found in microscopic images. Finally, more layers are added to form a full 3D model of a piece of cardiac tissue. The arrangement of gap junctions associated with a single myocyte is depicted in the lower part of Fig. 1. All the faces perpendicular to the fibre direction are assumed to contain gap junctions, and, in the model these faces touch the next layer of cells, assuring a cell-to-cell conduction through the intracellular space. Briefly, the myocytes had elongated, irregular shapes (FORBES and SPERELAKIS, 1995) that the model captured by varying the degree of elongation of the hexagons into columns. We coupled neighbouring cells end to end by means of gap junctions located at the irregular ends of each myocyte. A recent study by JAIN *et al.* (2003) using confocal microscopy showed a similar distribution of gap junction proteins. We assigned to each gap junction a resistance that matched experimental studies of cell-to-cell resistivities.

The inhomogeneities in the extracellular space stem from its division into capillaries and interstitial space. At the microscopic scale of our simulations, blood cannot be considered as a homogeneous medium; its composition of red blood cells and blood plasma must be taken into account. Measurements of the conductivity of blood at different haematocrit levels indicate that the red blood cells do not conduct, and that the blood plasma is the actual conductive medium (TRAUTMAN and NEWBOWER, 1983). As the size of a red blood cell is approximately equal to the cross section of a capillary, it will block the conducting pathway along the capillary.

To scrutinise the conductivity of capillaries, a detailed model of a capillary was constructed. In this model, the capillary has been split into three sections, the capillary wall, the blood cells and the blood plasma, and a fourth compartment representing the interstitial space surrounding the capillary; see Fig. 2. Measurements of blood flowing through small capillaries indicate that at least 90% of the capillary cross-section is blocked by the red blood cells (CHIEN *et al.*, 1984); hence, this lower limit was used in the model of the capillary. As we were investigating the bulk conductivity of cardiac tissue, it was assumed that the extracellular current had been distributed between the interstitial space and the blood within the capillaries. The model was used to predict the percentage of current flowing within the blood plasma of the capillary with respect to the total current flowing through the extracellular space. Assuming an externally applied electric field along the capillary, the currents were computed using a finite element model. In this model, the extracellular fluid conductivity was assumed to be 2.0 S m^{-1} (FOSTER and SCHWAN, 1989); the same value was taken for the blood plasma, and the capillary wall was assumed to be at least 50 times less conductive than both fluids. The red blood cells were assumed to be non-conducting. Assuming this configuration, the effective conductivity of the capillary (wall plus blood) was estimated as a function of the haematocrit. The results are displayed in Fig. 2. The results indicate that, for haematocrit values as low as 15%, the net conductivity of the capillary is significantly lower than the conductivity of the interstitial space, which is 2.0 S m^{-1}. Therefore the capillaries were assumed to be non-conducting in the model.

Another essential assumption of the model was that the cell membrane conductivity was negligible under the conditions of

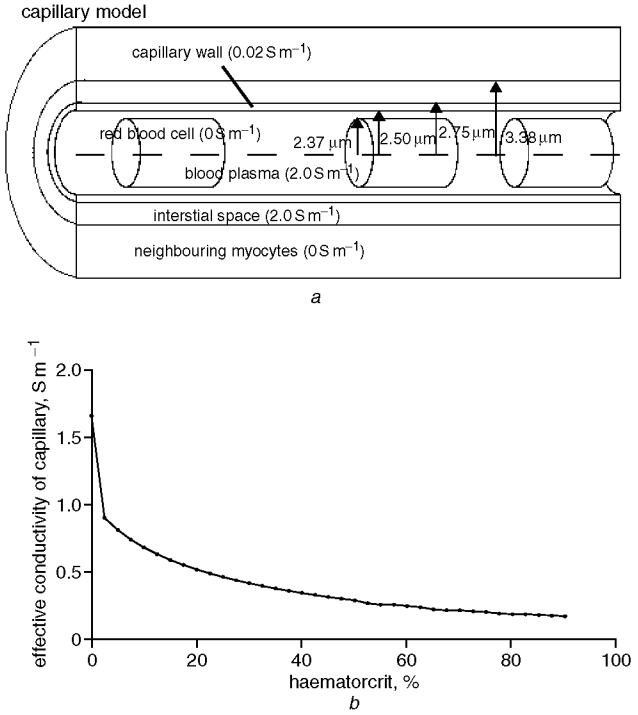

Fig. 2 *(a) Illustration of model used to assess effective conductivity of capillary. Figure depicts different components of model and radii used. (b) Effective conductivity of capillary as function of haematocrit*

the simulation, which treated the tissue as a passive volume conductor. For healthy tissue, this assumption resulted in computed values that were in good agreement with the effective intra- and extracellular conductivities reported in literature (STINSTRA *et al.*, 2005). A second justification for assuming a non-conducting membrane is that the resulting values are intended for use in bidomain simulations, which already explicitly includes the behaviour of the membrane.

Another importance facet of the model was that it was meant to represent a small tile in a much larger piece of myocardium. At the spatial resolution required to capture the role of cellular geometry, it was feasible only to create models on the scale of 20–100 cells, which we felt was adequate to capture realistic bulk behaviour. To allow replication of as many such tiles as the computation required (or permitted), we designed the edges of each to fit precisely with additional tiles in all directions.

To avoid the distorting effects of edges in the model, we adjusted conditions at the boundaries to meet two conditions

(i) A current exiting at one boundary node entered the model at the opposite boundary node
(ii) the potential at a node of the boundary was set equal to the potential of its counterpart on the opposite boundary.

To simulate the application of an external electric field to the tissue, we altered the second condition for node pairs that aligned with the externally applied potential, which we determined from the desired strength of electrical field multiplied by the thickness of the tissue.

The effective conductivities were obtained by computing the total amount of current flowing through the piece of tissue in a certain direction. The latter was calculated using the finite element method using a mesh consisting of tetrahedrons that was created on top of the geometric model. The effective conductivities σ_e and σ_i then became

$$\sigma_e = J_{ECS}/E_{app} \qquad \sigma_i = J_{ICS}/E_{app} \tag{1}$$

where J_{ECS} and J_{ICS} were the computed averaged current densities for the two compartments for a given direction, and E_{app} was the applied electric field.

The models used for this study consisted of of approximately 1.4 million elements in the intracellular space and 600 000 elements in the extracellular space, representing a cluster of $4 \times 4 \times 4$ myocytes (64 cells).

2.2 *Choice of model parameters*

Table 1 contains the parameters derived in a previous study (STINSTRA *et al.*, 2005) to represent the healthy condition. We assumed the conductivitiy of all compartments to be ohmic and assigned conductivity based on studies in the literature. The value of 2.0 S m^{-1} for interstitial conductivity corresponds to the conductivity of many extracellular fluids in the body (FOSTER and SCHWAN, 1989; SCHWANN and KAY, 1956; STINSTRA and PETERS, 2002). Values for the effective conductivity of the myocyte contents, 0.3 S m^{-1} along the fibre direction and 0.15 S m^{-1} across, were estimated based the layout of myofibrils and mitochondria and the mobility of potassium in the remaining space of the cytoplasm (STINSTRA *et al.*, 2005). The longitudinal conductivity value seemed to agree with measurements performed by BROWN *et al.* (1981) when corrected for temperature (STINSTRA *et al.*, 2005); in the model, we assumed a temperature of 37°C.

The model did not contain individual gap junction connections but rather modelled them by means of an effective surface resistance linking two adjacent cells. We assumed that the gap junctions were located at the ends of the processes of the individual myocytes. Measurements by Metzger and Weingart (WEINGART, 1986; METZGER and WEINGART, 1985) show an effective cell-to-cell resistance of about 1 M Ω after the value is corrected for the access resistance due to the resistance of the myocyte itself. As, in these measurements, not all these processes overlap, it was assumed that about half the processes overlap; hence, we chose a value for the effective gap junction surface resistivity of 1 M Ω spread out over half of the cross-section of a myocyte (STINSTRA *et al.*, 2005).

Addressing the goals of this study required changes in some model parameters to reflect increasing degrees of ischaemia and the passage of time from the onset of that ischaemia. To replicate the early decrease in conductivity described by KLÉBER and RIEGGER (1987), we altered the size of the capillaries to simulate the drainage of the interstitial space. As the capillary space in our model was non-conducting, this simulated both the shift of fluids into the capillary space and drainage of fluids out of the ischaemic volume. We represented the subsequent response to ischaemia by allowing the

Table 1 Overview of parameters used in conductivity model (healthy tissue)

Parameter	Value
Cytoplasm longitudinal conductivity	0.3 S m^{-1}
Cytoplasm transverse conductivity	0.15 S m^{-1}
Interstitial conductivity	2.0 S m^{-1}
Capillary wall conductivity	0.02 S m^{-1}
Blood plasma conductivity	2.0 S m^{-1}
Haematocrit	50%
Gap-junction resistivity	1.45×10^{-4} Ωm^2
Cell membrane resistivity	$+\infty$ Ωm^2
Average cell cross-section	290 μm^2
Average cell length	95 μm
Volume fraction myocytes	84%
Volume fraction interstitial space	11%
Volume fraction capillaries	5%

myocytes in the model to expand while maintaining their original spacing and organisation. Finally, to simulate the progressive electrical uncoupling of cells by the gap junctions, we increased the effective gap junctional resistance in the model from its nominal value.

3 Results

Using the parameters in Table 1, we obtained previously (STINSTRA *et al.*, 2005) an effective intracellular conductivity of 0.16 S m^{-1} (longitudinal) and 0.005 S m^{-1} (transverse) and an effective extracellular conductivity of 0.21 S m^{-1} (longitudinal) and 0.05 S m^{-1} (transverse).

To predict the changes in the bidomain conductivities under ischaemic conditions, we performed three series of simulations under the following conditions:

(a) an expansion of the capillaries in the ECS
(b) cell swelling
(c) the closure of the gap junctions.

The first two of these simulation series mainly affected the bidomain conductivities in the extracellular space, shown in Fig. 3. In the first simulation, capillary volume ranged from 30 to 50% of the ECS. At 50%, the capillaries occupied the maximum amount of the ECS possible while maintaining the cell spacing, and the remaining volume consisted of thin sheets of fluid separating the capillaries from surrounding myocytes. This increase in capillary volume resulted in a noticeable reduction in the effective longitudinal extracellular conductivity (from 0.21 S m^{-1} to about 0.17 S m^{-1}) and the anisotropy ratio (from 5.5 to 3.9), but hardly altered the effective transverse extracellular conductivity (from 0.046 S m^{-1} to 0.042 S m^{-1}).

The second simulation series, shown in Fig. 3*b*, shows the effect of cell swelling by increasing the size of each myocyte while maintaining a constant arrangement of myocytes, such that myocyte volume increased to 2.5 times the original value. In this simulation, the overall size of the model was inflated equally in all three dimensions, while the absolute dimensions of the distance between the myocytes were kept constant, thereby reducing the ECS volume fraction. Over this range of swelling, extracellular longitudinal conductivity changed from about 0.2 to 0.11 S m^{-1}.

To simulate the effect of gap junction closure, we carried out simulations in which the gap junction surface resistance varied from 1.45×10^{-4} Ωm^2 (healthy case) to 1.45×10^{-3} Ωm^2 (ischaemia). This change only affected the intracellular conductivities, which are depicted in Fig. 4, and resulted in an initially sharp decrease in conductivity. Because the transverse conductivity was affected more by the increase in the gap junctional resistance than the longitudinal, the intracellular anisotropy factor also increased in a non-linear fashion. For cell-to-cell resistances over 1.45×10^{-3} Ωm^2, the gap junctional resistance became the dominant factor in both the transverse and the longitudinal effective intracellular conductivities, which resulted in an anisotropy factor in the range of 50–60.

4 Discussion

One of the main motives for creating a model of cardiac conductivity was to estimate the changes in conductivity that arise during the various phases of ischaemia. Experimental data regarding these changes are especially sparse. One problem encountered in estimating the conductivity of ischaemic cardiac tissue is that ischaemia is a cascade of different processes taking place simultaneously or overlapping in time, so that there is no single static conductivity value for ischaemic tissue. Hence, in relating the changes in cardiac conductivity to the underlying changes in physiological state, understanding these different stages, their interactions and their implications becomes critical.

At the onset of ischaemia, there is a sudden increase in the longitudinal extracellular conductivity (SMITH *et al.*, 1995; KLÉBER and RIEGGER, 1987), and one hypothesis for this behaviour is capillary swelling resulting from draining of the interstitial fluid out of the tissue after the loss of capillary hydrostatic pressure. To evaluate this hypothesis, we simulated

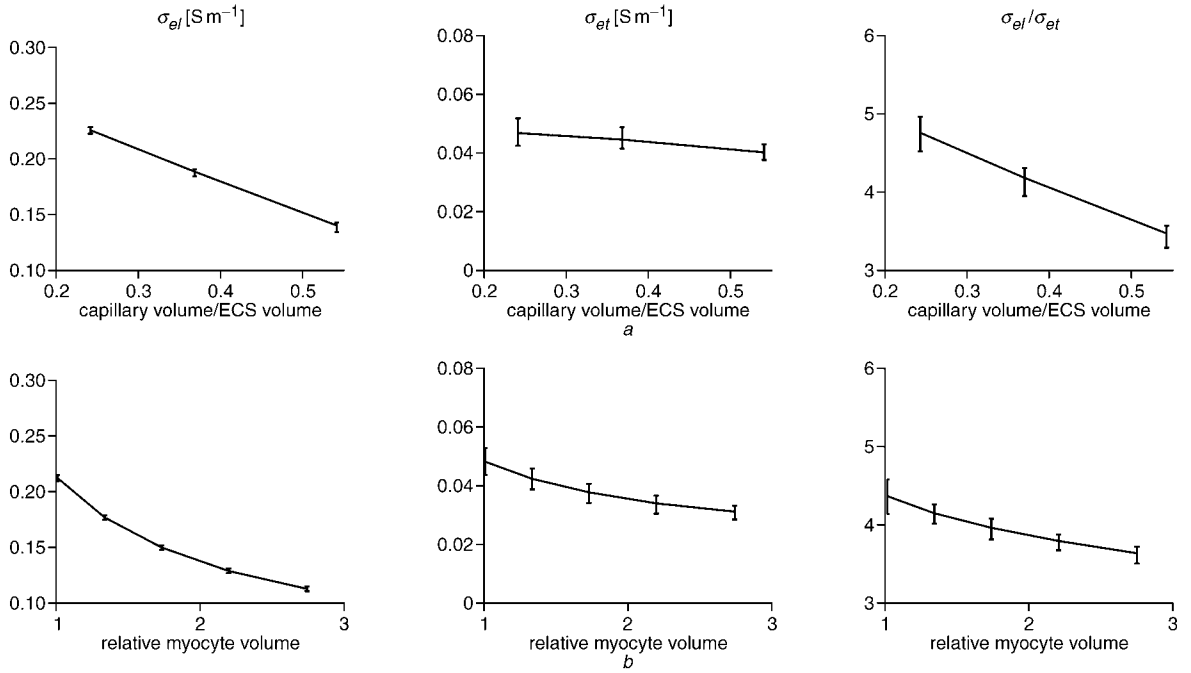

Fig. 3 *Effective extracellular conductivity as function of changes in morphology of ECS. (a) Changes due to swelling of capillaries; (b) effect of myocyte swelling. Error bars indicate maximum and minimum values found for effective conductivities. First column displays longitudinal effective conductivity; second column displays effective transverse conductivity; third column displays anisotropy ratio*

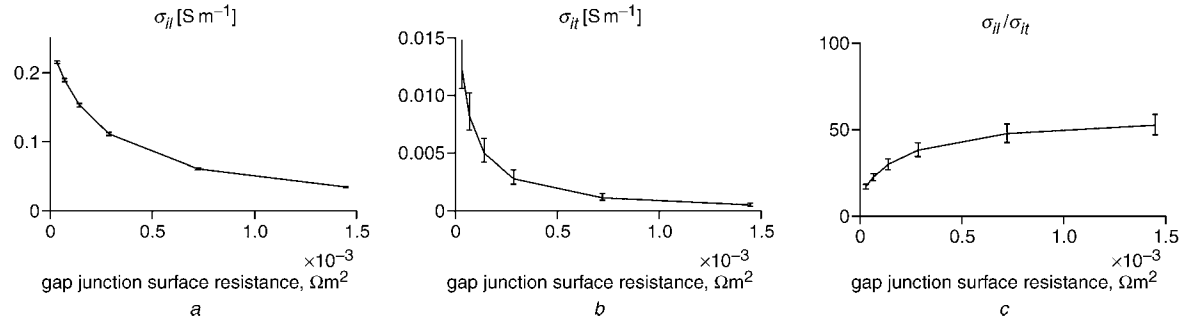

Fig. 4 *Effective intracellular conductivity as function of gap junction cell-to-cell surface resistance. Error bars indicate maximum and minimum values found for effective conductivities. (a) Longitudinal effective conductivity; (b) effective transverse conductivity; (c) anisotropy ratio*

the swelling of the capillaries (Fig. 2*a*), from a control state in which they occupied about 30% of the ECS to a state in which they occupied 50% of the ECS. Simulations of this transition showed a reduction in the extracellular conductivity of 20–25%, a value reasonably close to the measured reduction in the extracellular longitudinal conductivity of about 35% (KLÉBER and RIEGGER, 1987). A more realistic response would be at least some drainage of interstitial fluid through the capillaries out of the ischaemic region, and therefore somewhat less capillary swelling, but the latter effect would still be a loss of interstitial fluid and, hence, the increased extracellular resistance.

The additional decrease in extracellular conductivity during the next phase of ischaemia, described by Smith *et al.*, probably arises as a result of cell swelling (SMITH *et al.*, 1995). We were able to replicate the small reduction in extracellular conductivity that they reported by allowing the cells in the model to swell by 8–16%, a range reported in the literature (TRANUM-JENSEN *et al.*, 1981; STEENBERGEN *et al.*, 1985). The decrease in conductivity in this phase was not as large as that immediately following ischaemia, which seems to match the time curve of resistance in ischaemia reported in the literature (KLÉBER and RIEGGER, 1987; JAIN *et al.*, 2003; OWENS *et al.*, 1996; SMITH *et al.*, 1995).

A further factor that influences tissue conductivity during ischaemia is the reduction in the intracellular conductivity that arises because of a graded failure in the gap junctions. To replicate the results of Smith *et al.*, which showed a two-step rise in the longitudinal bulk resistivity, at first 1.5-fold and then levelling off at a 2.7-fold overall increase, would require a decrease in the longitudinal bulk conductivity from 0.38 S m^{-1} to about 0.14 S m^{-1}. In combination with the reduction in conductivity for the extracellular space of 40% (cell swelling and collapse of the interstitial space) described above, this would require a much larger drop in the intracellular conductivity, which lies effectively in parallel with the extracellular conductivity. We simulated a tenfold increase in gap junction resistivity, which effectively made the extracellular conductivity the major contributor to the bulk conductivity. Under these conditions, the extracellular longitudinal conductivity was 0.14 S m^{-1} and the intracellular conductivity was 0.03 S m^{-1}, resulting in a bulk longitudinal conductivity of 0.17 S m^{-1}, which is close to the 0.14 S m^{-1} value observed by SMITH *et al.* (1995). The actual increase in the gap junction resistivity is hard to estimate from current literature. However, a recent study by JAIN *et al.* (2003) showed that, when cardiac tissue was subjected to 30 min of no-flow ischaemia, the density of connexin-43 proteins in the cell membranes was reduced to 10–20% of the original density. This near tenfold decrease can be correlated to the tenfold increase in the cell-to-cell resistance needed to match the range of conductivity values reported by SMITH *et al.* (1995).

In the present study, we assumed that the capillaries are non-conducting, whereas in reality they conduct some current. Although the capillary wall and red blood cells make the effective conductivity of a capillary lower than the effective one of the interstitial space, some current will still flow through this domain. One effect we did not consider is that the capillaries, after an initial swelling phase, may transport the interstitial fluid to other parts of the heart. This could result in a subsequent collapse of the capillaries, and, if they contributed slightly to the extracellular conductivity in the healthy case, this effect may further increase the change in the extracellular conductivity during ischaemia.

We did not include the well-documented effect of elevated extracellular potassium concentration in the simulations of ischaemic conductivity (YAN *et al.*, 1996). Even with a typical elevation of potassium, the dominant extracellular ions remain sodium and chloride, such that the effect on electrolyte conductivity is likely to be negligible (less than 5%).

Acknowledgment—This research would not have been possible without the generous support of the National Institutes of Health BISTI grant P20 HL68566-01.

References

BEARDSLEE, M. A., LERNER, L. D., TADROS, P. N., LAING, J. G., BEYER, E. C., YAMADA, K. A., KLÉBER, A. G., SCHUESSLER, R. B., and SAFFITZ, J. E. (2000): 'Dephosphyorylation and intracellular redistribution of ventricular connexin43 during electrical uncoupling induced by ischemia', *Circ. Res.*, **87**, pp. 656–662

BROWN, A. M., LEE, K. S., and POWELL, T. (1981): 'Voltage clamp and internal perfusion of single rat heart muscle cells', *J. Physiol.*, **318**, pp. 455–477

CARMELIET, E. (1999): 'Cardiac ionic currents and acute ischemia: from channels to arrhythmias', *Physiol. Rev.*, **79**, pp. 917–1017

CHIEN, S., USAMI, S., and SKALAK, R. (1984): 'Blood flow in small tubes', in RENKIN, E. M., and MICHEL, C. C. (Eds) '*Handbook of physiology, section 2, The cardiovascular system, volume IV, Microcirculation part I*' (American Physiological Society, Bethesda, Maryland, 1984), pp. 217–249

CINCA, J., WARREN, M., CARRENO, A., TRESANCHEZ, M., ARMADANS, L., GOMEZ, P., SOLER-SOLER, J. (1997): 'Changes in myocardial electrical impedance induced by coronary artery occlusion in pigs with and without preconditioning', *Circ.*, **96**, pp. 3079–3086

DUFFY, H. S., ASHTON, A. W., O'DONNELL, P., COOMBS, W., TAFFET, S. M., DELMAR, M., and SPRAY, D. C. (2004): 'Regulation of Connexin43 protein complexes by intracellular acidification', *Circ. Res.*, **94**, pp. 215–222

FLEISCHHAUER, J., LEHMANN, L., and KLÉBER, A. G. (1995): 'Electrical resistances of interstitial and microvascular space and determinants of the extracellular electrical field and velocity of propagation in ventricular myocardium', *Circ.*, **92**, pp. 587–594

FORBES, M. S., and SPERELAKIS, N. (1995): 'Ultrastructure of mammalian cardiac muscle', '*Physiology and pathophysiology of the heart*, 3rd edn' (Kluwer Academic Publishers, Norwell, MA, 1995), chap. 1, pp. 1–35

FOSTER, K. R., and SCHWAN, H. P. (1989): 'Dielectric properties of tissues and biological materials: a critical review', *Crit. Rev. Biomed. Eng.*, **17**, pp. 25–104

HENRIQUEZ, C. S., TRANQILLO, J. V., WEINSTEIN, D. M., HSU, E. W., and JOHNSON, C. R. (2004): '*Three-dimensional propagation in mathematic models: integrative model of the mouse heart*' (Saunders Company, Philadelphia, 2004), chap. 30, pp. 273–281

HOPENFELD, B., STINSTRA, J. G., and MACLEOD, R. S. (2004): 'A mechanism for ST depression associated with contiguous subendocardial ischemia', *J. Cardiovasc. Electrophysiol.*, **15**, pp. 1200–1206

HOPENFELD, B., STINSTRA, J. G., and MACLEOD, R. S. (2005): 'The effect of conductivity on ST-segment epicardial potentials arising from subendocardial ischemia', *Ann. Biomed. Eng.*, **33**, pp. 751–763

ROTH, B. J. (2004): '*Two-dimensional propagation in cardiac muscle*' (Saunders Company, Philadelphia, 2004), chap. 29, pp. 267–272

JAIN, S. K., SCHUESSLER, R. B., and SAFFITZ, J. E. (2003): 'Mechanisms of delayed electrical uncoupling induced by ischemic preconditioning', *Circ. Res.*, **92**, pp. 1138–1144

KLÉBER, A. G., and RIEGGER, C. B. (1987): 'Electrical constants of arterially perfused rabbit papillary muscle', *J. Physiol.*, **385**, pp. 307–324

METZGER, P., and WEINGART, R. (1985): 'Electric current flow in cll pairs isolated from adult rat hearts', *J. Physiol.*, **366**, pp. 177–195

OWENS, L. M., FRALIX, T. A., MURPHY, E., CASCIO, W. E., and GETTES, L. S. (1996): 'Correlation of ischemia-induced extracellular and intracellular ion changes to cell-to-cell electrical uncoupling in isolated blood-perfused rabbit hearts', *Circ.*, **94**, pp. 10–13

SACHSE, F. B. (2004): '*Computational cardiology: modeling of anatomy, electrophysiology, and mechanic*' (LNCS 2966, Springer Press, Heidelberg, 2004)

SCHWANN, H. P., and KAY, C. F. (1956): 'The conductivity of living tissues', *Ann. N.Y. Acad. Sci.*, **65**, pp. 1007–1013

SMITH, W. T., FLEET, W. F., JOHNSON, T. A., ENGLE, C. L., and CASCIO, W. E. (1995): 'The Ib phase of ventricular arrhythmias in ischemic in situ porcine heart is related to changes in cell-to-cell electrical coupling', *Circ.*, **92**, pp. 3051–3060

STEENBERGEN, C., HILL, M. L., and JENNINGS, R. B. (1985): 'Volume regulation and plasma membrane injury in aerobic, anaerobic, and ischemic myocardium *in vitro*', *Circ. Res.*, **57**, pp. 864–875

STINSTRA, J. G., HOPENFELD, B., and MACLEOD, R. S. (2004): 'Using models of the passive cardiac conductivity and full heart anisotropic bidomain to study the epicardial potentials in ischemia'. Proc., 26th Annual Int. Conf. of the IEEE Engineering in Medicine and Biology Soc., (2), pp. 3555–3558

STINSTRA, J. G., HOPENFELD, B., and MACLEOD, R. S. (2005): 'On the passive cardiac conductivity', *Ann. Biomed. Eng.*, **33**, pp. 1743–1751

STINSTRA, J. G., and PETERS, M. J. (2002): 'The influence of fetoabdominal tissues on fetal ECGs and MCGs', *Arch. Physiol. Biochem.*, **110**, pp. 165–176

TRANUM-JENSEN, J., JANSE, M. J., FIOLET, J. W. T., KRIEGER, W. J. G., D'ALNONCOURT, C. N., and DURRER, D. (1981): 'Tissue osmolality, cell swelling, and reperfusion in acute regional myocardial ischemia in the isolated porcine heart', *Circ. Res.*, **49**, pp. 364–381

TRAUTMAN, E. D., and NEWBOWER, R. S. (1983): 'A practical analysis of the electrical conductivity of blood', *IEEE Trans. Biomed. Eng.*, **30**, pp. 141–153

WEINGART, R. (1986): 'Electrical properties of the nexal membrane studied in rat ventricular cell pairs', *J. Physiol.*, **370**, pp. 267–284

WRIGHT, A. R., and REES, S. A. (1998): 'Cardiac cell volume: crystal clear or murky waters? A comparison with other cell types', *Pharmacol. Ther.*, **80**, pp. 89–121

YAN, G. X., CHEN, J., YAMADA, K. A., KLÉBER, A. G., and CORR, P. B. (1996): 'Contribution of shrinkage of extracellular space to extracellular K+ accumulation in myocardial ischemia of the rabbit', *J. Physiol.*, **490.1**, pp. 215–228

Authors' biographies

JEROEN STINSTRA is a Postdoctoral Fellow at the Cardiovascular Research & Training Institute and the Scientific Computing & Imaging Institute at the University of Utah. He obtained his PhD degree in Applied Physics from Twente University in the Netherlands, in 2001, where he worked at the BioMagnetic Center, Twente. The goal of Dr Stinstra's research is to advance the understanding of eletrophysiology in the heart using a combination of modelling and experimental approaches.

SHIBAJI SHOME obtained his Bachelor's degree in Medical Electronics Engineering from BMS College of Engineering, Bangalore University, India, in 1999. He is presently a PhD student in Bioengineering and works as a Research Assistant at CVRTI. His interests include cardiac electrophysiology, visualisation and modelling of ischaemia biophysics.

BRUCE HOPENFELD received the BS degree, in 1989, from the University of California at Los Angeles. In 1993, he received the JD degree from the University of Chicago. From 1993 to 2000, he was a practising Attorney. In 2004, he received the PhD degree in Bioengineering from the University of Utah. He is currently a Postdoctoral Fellow at the Laboratory of Cardiac Energetics, National Heart, Lung & Blood Institute, National Institutes of Health, in Bethesda, Maryland.

ROB MACLEOD trained in physics, electrical engineering and physiology and is an Associate Professor at the University of Utah. His academic appointments are in Bioengineering and Internal Medicine (Cardiology), and he is an Associate Director of the Scientific Computing & Imaging Institute and the Cardiovascular Research & Training Institute. He is the Co-director of the NIH-funded Center for Bioelectric Field Modeling, Simulation & Visualization at Utah and an investigator on several other interdisciplinary programs. The goal of Dr MacLeod's own research is to bring theoretical, computational and experimental techniques to bear on problems of cardiac electrophysiology. He has also created computational tracks in both the graduate and undergraduate programs in Bioengineering at Utah and is the Director of these programs.